Verification of HIRLAM with ECMWF physics compared with HIRLAM reference versions

Cisco de Bruijn and Erik van Meijgaard*

February 2, 2005

Abstract

ECMWF physics has been successfully ported into the HIRLAM system, version 5.0.6. Model integrations have been carried out in the reference framework at 0.5 degree horizontal resolution for the month December 1999 and a 14-day period in May 2000. Relative to the reference HIRLAM version 5.0.6, verification scores of near-surface parameters range from neutral in the Spring period to significantly better in the Winter period. In particular, the forecast of the mean sea level pressure during a stormy episode is found to improve considerably. A similar conclusion holds for the comparison with the more recent HIRLAM version 5.1.4, which includes the land surface scheme ISBA, but differences in the scores are generally smaller. A considerable diurnal oscillation in the bias of the 2 meter temperature produced by HIRLAM with ECMWF physics and HIRLAM version 5.0.6 is found greatly reduced in HIRLAM version 5.1.4, most likely owing the assimilation of the surface parameters that was introduced with the land surface scheme ISBA. Verification of 10-meter wind speeds over the southern North Sea basin show that all model three model versions, and in particular HIRLAM with ECMWF physics, underpredict the number of high wind speed events over sea. Verification of upper air parameters shows comparable results among the three model versions. Verification scores of 6-hour precipitation show that HIRLAM with ECMWF physics is performing consistently better both in amounts of precipitation as in the occurrence of events with either high or low amounts of precipitation. Finally, a case study of a multi-day extreme rainfall event over parts of Italy has been conducted to demonstrate the feasibility of HIRLAM with ECMWF physics to produce useful precipitation forecasts at fine horizontal resolution (11 km).

*Royal Netherlands Meteorological Institute KNMI, P.O. Box 201, 3730 AE De Bilt, Netherlands (cisco.de.bruijn@knmi.nl;vanmeijg@knmi.nl).

Contents

1 Introduction **3**

2 Model description **3**
2.1 HIRLAM 5.0.6 + ECMWF physics (PHEC) . . . 3
2.2 HIRLAM 5.0.6 (HL506) . . . 5
2.3 HIRLAM 5.1.4 (HL514) . . . 6
2.4 Experimental setup . . . 6
2.5 Method of verification . . . 7

3 Results **8**
3.1 Surface verification . . . 8
3.1.1 Mean sea level pressure . . . 8
3.1.2 10m Wind . . . 8
3.1.3 2m Temperature . . . 10
3.1.4 2m Relative humidity . . . 11
3.2 Upper air verification . . . 11
3.3 Precipitation . . . 12
3.3.1 55 km model . . . 12
3.3.2 11 km model . . . 14
3.4 Other experiments . . . 15
3.4.1 HIRLAM radiation and CPU demand . . . 16
3.4.2 The role of soil moisture capacity . . . 17

4 Conclusions and discussion **17**

5 Acknowledgements **18**

6 Appendix: Overview of Technical Implementation **19**

1 Introduction

In contribution to the HIRLAM-5 project the ECMWF parameterization package of physical processes has been ported into the HIRLAM forecast component. Such a system is expected to provide a platform in which the HIRLAM community can more easily and more directly benefit from research and development at the ECMWF. Furthermore, it offers the possibility to objectively inter compare the physics components of HIRLAM and ECMWF in a LAM oriented framework. HIRLAM 5.0.6 was taken as the reference version. The ECMWF physics has been adopted from release CY23R4, which also served as the basis for the ERA40 project. The forecast component of the new model has been adopted by the Atmospheric Research division at KNMI for the purpose of regional climate modeling. In that context the model is referred to as RACMO2 (Regional Atmospheric Climate Model, version 2).
For the comparison, the model has been operated in NWP-mode involving an assimilation-forecast cycle. The model output is examined using the standard verification package of the HIRLAM system. The performance of the NWP model is given in terms of bias and standard deviation. Results are also compared with a more recent version of HIRLAM version 5.1.4 which operates the land surface scheme ISBA.
For the purpose of verifying short-term integrations of the new model in NWP-mode none of the components or parameter settings in the ECMWF physics package have been altered. However, a recent assessment of the quality of RACMO2 operated for present-day climate conditions revealed some serious shortcomings (Lenderink et al., 2003).

2 Model description

In Table 1 an overview is given of the model versions used in this study. Hereafter HIRLAM 5.0.6 + ECMWF physics, HIRLAM 5.0.6 and HIRLAM 5.1.4 are referred to as PHEC, HL506 and HL514, respectively. The analysis, initialization and dynamics are similar for all three models versions and are described in Undén et al. 2002 [19]. It is also clear that the differences between HL506 and HL514 focus on the treatment of the surface parameters.

2.1 HIRLAM 5.0.6 + ECMWF physics (PHEC)

The physical package of the ECMWF model version CY23R4 was adopted and embedded in HL506. Details on the concept and the technical implementation can be found in Newsletter 38 [9]. Additionally, an extensive description of the physical package itself can be found in [21]. Here we provide a brief overview of the major components which form part of this package. At first the tendencies due to radiative transfer are calculated (Morcrette [10]), secondly the turbulent diffusion scheme is solved which accounts for

	HIRLAM 5.0.6	HL5.0.6+ECMWF physics	HIRLAM 5.1.4
References	Undén et al, 2002	Van Meijgaard, 2001	Undén et al, 2002
Analysis	OI	OI	OI
Surface Analysis	no	no	yes
Lateral boundaries	ECMWF 6h	ECMWF 6h	ECMWF 6h
Initialization	DFI	DFI	DFI
Dynamics	SL 720/120s	SL 720/120s	SL 720s
Resolution	0.5/0.1 deg	0.5/0.1 deg	0.5 deg
Radiation	Savijärvi, 1990	Morcrette, 1991	Savijärvi, 1990
Convection	Kuo, 1965	Mass flux, Tiedtke, 1989	Kuo, 1965
Clouds	STRACO Sass et al, 1999	Progn cloud scheme Tiedtke, 1993	STRACO Sass et al, 1999
Turbulence	TKE-closure Cuxart et al, 2000	K-closure Louis, 1979	TKE-closure Cuxart et al, 2000
Surface scheme	no tiles Källén, 1996	TESSEL Van den Hurk et al, 2000	ISBA Noilhan et al, 1996

Table 1: *Overview model versions, OI means Optimal Interpolation, DFI is Digital Filtering Initialization, SL is Semi Lagrangian advection scheme, TKE stands for Turbulent Kinetic Energy*

exchange processes in the atmospheric boundary layer using Monin-Obukhov similarity [5], deep convection is parameterized by means of a mass flux scheme with a CAPE closure formulation [16], subsequently cloud and precipitation processes are integrated by the prognostic cloud scheme [17], finally the soil processes are treated with a tiled surface soil scheme, known as TESSEL (Tiled ECMWF Scheme for Surface Exchanges over land) [20].

This land surface model employs four soil layers (0.07m, 0.21m, 0.72m, 1.89m) where the top three layers cover most of the root zone for all vegetation types. To calculate the exchange of heat, moisture and momentum at the interface of surface and atmosphere in the tiled formulation, each grid-box is divided into fractions (tiles), with up to six fractions over land (bare ground, low and high vegetation, intercepted water, shaded and exposed snow) and up to two fractions over sea and freshwater bodies (open and frozen water). Each fraction has its own properties defining separate heat and water fluxes used in an energy balance equation in order to solve for the tile skin temperature. Sensible and latent heat flux are parametrized by resistance based formulations. Soil heat budget is calculated based on the Fourier diffusion law. Tiled flux information is aggregated over the entire grid box in order to integrate the atmospheric profiles of temperature, moisture

and momentum.

ECMWF physics expects its own surface characteristics and as such a couple of additional fields need to be specified in the creation of climate files. The land surface scheme expects parameters to describe type and degree of low and high vegetation. In addition to the roughness length for momentum also a roughness length for heat is needed. It was given preference for reasons of consistency to prepare the roughness length fields according to the prescription in the IFS documentation [21]. As such the roughness length associated to vegetation prepared in the creation of climate files is blended with information on sub-grid scale orographic variance. The orographic wave drag scheme requires topographic information on the variance of terrain height, and, in addition, on anisotropy, mean slope, and direction of largest gradient. This is also taken care of in the creation of climate files. Information to prescribe surface characteristics has been taken from various sources. The surface roughness lengths for momentum, heat and moisture are calculated following the description in the IFS documentation (see [21], paragraph 9.5).

No actual analysis of surface parameters is carried out. Data from the previous run (first guess) are taken to provide initial values for the model integrations. At the start of the first run of each experiment they are derived from the driving (ECMWF) model.

2.2 HIRLAM 5.0.6 (HL506)

In the physics the radiative fluxes are calculated according to Savijärvi [15]. This scheme describes with sufficient accuracy the radiative processes in the troposphere. The scheme is fast and is called every time step, which allows describing radiation associated with short time fluctuating cloud cover. The vertical transport is governed by a Kuo type convection scheme [8] with a moisture convergence closure. Although this scheme has been designed for the tropics, it has been adapted successfully for mid latitudes. The STRACO scheme [14] (Soft TRAnsistion COnvection) parameterizes both large scale and convective condensation and puts emphasis in achieving gradual transitions between both regimes. Despite the theoretical short comings of the Kuo type convection scheme, STRACO has proven its value in practice. The turbulence scheme is based on prognostic turbulent kinetic energy combined with a diagnostic length scale. This approach describes the entrainment at the top of the ABL adequately and is also suitable for high resolutions. The surface scheme (Källén, 1996) [6] describes the evolution of soil temperature, soil water content and snow depth over land or ice. The grid box may be either land, sea or a mixture of land and sea and ice. The soil is represented by three layers. The surface fields are initialized to the first guess values from the previous forecast. If no forecast is available the information is taken from climatology.

2.3 HIRLAM 5.1.4 (HL514)

HL514 utilizes for a great deal the same physics as HL506. The new features are the ISBA (Interaction Soil Biosphere Atmosphere) surface scheme and the analysis of surface variables. ISBA is a tile scheme which allows different bottom types within the grid box. The scheme is described by Noilhan and Planton, 1996 [11]. Five surface types are considered within each grid square: sea/lake water, ice, bare land, forest and low vegetation. The soil is divided in two layers: one surface layer, with a depth typically of 1 cm, that responds to the diurnal cycle, and a total layer extending down to a depth of about 1m following a time scale of some days. In each time step the sensible and latent heat fluxes from each sub grid surface are weighted according to their fractional share of the grid square to form the total surface fluxes. The aggregated fluxes are used at the lowest model level as lower boundary condition for the Atmospheric Boundary Layer (ABL) and radiation schemes.

The surface analysis initializes the following variables: sea surface temperature (SST), fraction of water and ice, 2-metre temperature, 2-metre relative humidity, surface soil temperature, mean soil temperature, surface soil water content and total soil water content. The soil water content analysis is based on a sequential method, which corrects water content depending on 2-metre temperature and relative humidity forecast errors, only in those synoptic cases where screen variables are strongly influenced by the surface beneath. Further details about the surface analysis can be found in Rodriguez et al., 2003 [12].

2.4 Experimental setup

In this study, model integrations are carried out at 0.5-degree horizontal resolution and with 31 layers in the vertical. The model domain, counting 114x100 grid points, covers Europe and a large part of the North Atlantic Ocean. The model is integrated with a semi-Lagrangian advection scheme employing a time step of 12 minutes. An optimal interpolation analysis is carried out every 6 hours; the forecast length is 48 hours. Lateral boundary conditions are inferred from ECMWF analyses and are updated every 6 hours. In a second experiment model integrations are also carried out at a 0.1-degree horizontal resolution. The model domain counting 114x100 grid points again, now covers mainly Italy. This domain is chosen to enable the use of high resolution rainfall observations in the Campania region (see Fig. 1). The observations are situated in the middle of the domain. The time step was adapted to 180 seconds and the analysis is carried out every 3 hours. The forecast length is 24 hours and the Lateral Boundary Conditions are inferred from ECMWF analyses and are updated every 6 hours.

Two periods with different weather regimes, i.e. 01-12-1999 to 31-12-1999 (December 1999) and 06-05-2000 to 23-05-2000 (May 2000), were selected to verify the models. December 1999 was a striking month because of its active cyclones. On 3 and 4 Decem-

ber Scandinavia was hit by Anatol, a deep low with wind gusts up to 52 m/s near Sylt (Denmark). On Boxing Day a heavy storm, called Lothar, crossed central Europe. The core pressure was 962 hPa, which is not particularly low for a mid-latitude depression. However, a spectacular drop in surface pressure of 21 hPa in 6 hours was observed in Brittany, France on 26 December around 06 UTC ([1]). Subsequently, Europe was hit by a third cyclone, named Martin, again causing considerable damage in France. During 14-18 December a heavy rain event occurred in the Campania region in Italy, causing torrential rain and heavy flooding.
May 2000 was a springtime period characterized by a blocked circulation in the beginning followed by a sudden transition to unsettled weather around 16 May. Of more general interest and typically occurring in spring is the pronounced diurnal cycle of 2m temperature and relative humidity.

2.5 Method of verification

Verification scores in terms of bias and standard deviation are given for mean sea level pressure, 10 meter wind, 2 meter temperature, relative humidity, dew point temperature and precipitation. Additionally, verification scores are calculated for geopotential height, wind, temperature, and relative humidity at standard levels in the atmosphere. The standard deviation is interpreted as the unbiased component of the root-mean-square error. To interpret the model results from another perspective, we constructed multi contingency tables. In this way we were able to assess the behavior of the models in the extremes. Moreover a diagnosis in terms of false alarms, misses and correct rejections became feasible.

In order to obtain general insight in the model performance it is common practice to look at the verification of the mean sea level pressure and the geopotential height. Both parameters are slowly varying and rather independent on local conditions. In contrast typical boundary layer parameters like 10 meter wind, 2 meter temperature and relative humidity are influenced by local conditions. Model predictions of near-surface parameters have been verified using SYNOP observations, available from a predefined list of stations in Europe, the so-called EWGLAM stations (Fig. 1) Predictions of upper-air parameters have been verified on the basis of all available TEMP observations in the model domain.

Prior to the actual verification a quality check is performed. The difference between the field and observation is used to obtain a quality estimate of the observation. If it deviates too much from the field, it will not be used for the verification. Grossly erroneous observations are thus avoided to improve the statistics. However a shortcoming of this method is that a high quality background field is required.

3 Results

3.1 Surface verification

The Figs 2 and 5 present the verification scores for December 1999 and for a 14-day period in May 2000, respectively. In these diagrams the standard deviation and bias are given as a function of the forecast length. The bias is an averaged value and might be affected by compensating errors. Therefore the diurnal cycle of the bias is studied in more detail by also plotting the bias on the synoptic main hours (00, 06, 12 and 18 UTC) as a function of the forecast length (see Figs 3 and 6). From these diagrams the diurnal cycle can be derived. For instance if the curves coincide, the bias is steady and there is no oscillating effect. However if the curves are above and below zero, the compensating error effect takes place when the different contributions are averaged in a single score as function of the forecast length. After these introductory remarks we will discuss the scores per verified variable in more detail.

3.1.1 Mean sea level pressure

The first test period, December 1999, shows an improvement in the bias and standard deviation of mean sea level pressure forecasts of PHEC relative to HL506 (Fig. 2). HL514 shows a less pronounced improvement compared to HL506. These differences can be explained by the ABL parameterization. HL506 and HL514 carry the CBR scheme ([2]), which tends to underestimate the amount of mixing in stable conditions (Tijm 2003 [18]). This leads to too little ageostrophic flow in depressions, causing too much deepening and too slow filling of depressions. This might explain the excessive large bias. No improvement is found for this parameter in the May 2000 verification period (Fig. 5). The bias is considerably smaller than in the first test period. From Fig. 3 (first column) it is clear that PHEC has the superior score in December 1999 with a negative bias which tends to level off, while the other models are progressively becoming more negative. As there is almost no diurnal oscillation in the surface pressure, there is hardly an oscillation visible in the bias. The other test period Fig. 6 (first column) shows that there is no clear trend in the surface pressure bias for all model versions.

3.1.2 10m Wind

For both periods the 10m wind speed bias reduces when PHEC and HL514 are applied, but the standard deviation hardly improves. Fig. 3 (2nd column) show diurnal oscillations in the bias of the wind speed. In the May period (Fig. 6) biases are alternating around zero, so averaging implies that positive contributions are evened out by negative values. In December the bias remains positive and at +48h it becomes 1m/s, while the standard deviation in PHEC is 2.5 m/s, which does not differ much from the other models.

Fig. 6 (2nd column) reveals a clear diurnal oscillation in the wind speed bias. All models show the largest positive bias at midnight (00 UTC) while it becomes negative at 12 UTC. In the winter period (with occurring high wind speeds) the bias remains positive and PHEC has the best result. Too strong vertical mixing under stable conditions is probably the cause for too high wind speed during the evening and night in spring and all day long in winter (see also De Rooy, 1993 [13]). For such a stormy period it is interesting to study the model performance of the extremes. We focus here on the wind speed for a small area at sea. This area is the Southern North Sea (SNS) and is depicted in Fig. 1. In this particular area there are 30 observations available on average.

In Fig. 8 observations and model results are presented, showing a frequency distribution in combination with an averaged scatter plot. The observations are binned over an interval of 0.5 m/s and matched with model predictions. All the bin-members are averaged to create a figure that shows the average predicted wind speed as a function of the observed wind speed. This shows if a model has the tendency to overpredict or underpredict certain wind speeds, although phase errors will lead to a deviation from the diagonal as low wind speeds can be forecasted at locations where high winds speeds are observed and viceversa. The number of model members are counted and given as a frequency distribution in Fig. 8 (upper panel). PHEC has the best performance in the lower wind regime. HL506/HL514 and PHEC utilize a very similar formulation of the roughness length over sea. At low wind speeds the roughness length scales with the kinematic viscosity and at high wind speeds it is based on the Charnock relation. Owing to a different choice of the Charnock coefficient, which is specified as 0.014 over open sea in HL506/HL514 and 0.018 in PHEC, and a somewhat different combination of the contribution from both wind speed regimes, the roughness length in PHEC turns out to be always larger than in HL506/HL514 for the entire wind speed range. This likely explains the somewhat smaller 10-meter wind speed found with PHEC compared to HL506/HL514. Note that none of the models is able to predict extreme high wind speeds. To study this in more detail we organize the data in a two category contingency table ($p \leq 16$ and $p > 16m/s$) and work out the occurrences in terms of hits, misses, false alarms and correct rejections. The hits correspond with observed YES and predicted YES, false alarm with observed NO and predicted YES, misses with observed YES and predicted NO and correct rejection with observed NO and predicted NO. From Table 2 it is confirmed that PHEC underperforms in forecasting extreme wind speeds. Surprisingly the control run (HL506) has a better result in this respect than HL514. The higher hit rate of HL506 is accompanied, however, by a somewhat higher false alarm rate.

The wind vectors, as depicted in Figs 2 and 5 (2nd row, 1st column) take in account errors in wind direction in relation to significant wind speeds. Note that in these diagrams only the rms value is presented. In May 2000 there is hardly any difference between the model versions. Over the stormy December period PHEC gives the best results.

	HL506	PHEC	HL514
hi	9.9	7.5	8.6
fa	6.1	3.1	5.1
mi	7.8	10.2	9.1
cr	76.2	79.2	77.2

Table 2: *Scores based on 2 categories ($p \leq 16$ and $p > 16m/s$), hi=hits, fa=false alarm, mi=miss, cr= correct rejection.*

3.1.3 2m Temperature

PHEC reveals an improvement in the bias for December. At first glance this looks like a positive outcome, but upon further examination of the bias, a profound diurnal cycle around zero is found (Figs 3 and 6).

	HL506	PHEC	HL514
hi	1.2	1.7	1.2
fa	2.0	1.5	1.9
mi	0.2	0.8	0.1
cr	96.6	96.0	96.7

Table 3: *Scores based on 2 categories ($p \leq -10$ and $p > -10°C$), hi=hits, fa=false alarm, mi=miss, cr= correct rejection.*

In May, the negative bias of the control run (HL506) becomes more negative when PHEC is applied for forecasts valid at 1800 UTC. At the other times there is a slight improvement. The positive bias at 00 UTC reduces slightly. Forecasts valid at 06 UTC hardly change, while the ones at 12 UTC improve slightly. Adding up these components leads to an overall better value of the bias, because of the beneficial effect of compensating errors. Moreover PHEC might also benefit from the skin layer which allows a quicker response to radiative forcing. HL514 becomes close to zero for larger forecast times and this reduction is also due to compensating, but smaller errors. However, close to the analysis time the bias is negative and increases slightly during the integration period. HL514 is found capable of substantially reducing the standard deviation of the temperature close to the analysis, which due to the surface analysis scheme which is carried out in HL514. However it is striking to see that the standard deviation grows with increasing forecast times. In Fig. 9 a scatter plot for modeled against observed temperature is presented. For low temperatures all models have a positive bias. To study this phenomenon in more

detail, we constructed contingency tables with the following classification: $p \leq -10$ and $p > -10$ °C (see Table 3). Note that only 4 % of the data belongs to this category. PHEC has the highest hit rate of 1.7 %, but also the highest miss rate of 0.8 %.

3.1.4 2m Relative humidity

Scores of dew point temperature and relative humidity at 2m are depicted in Fig. 2 (3rd row). At first sight PHEC reveals a good result in reducing the bias. However, on inspection of the time series (not shown) it becomes clear again that compensating errors play a role. Another reason to suspect the bias reduction is that the standard deviation hardly improves. During the May period (Fig. 5) the biases of all model versions deteriorate with increasing forecast times and become negative. Note that the standard deviation improves for the PHEC model version. To study the +24 forecast in December 1999 we give all

	HL506	PHEC	HL514
hi	15.3	21.1	16.5
fa	8.7	14.2	9.3
mi	18.5	12.8	17.2
cr	57.5	51.9	57.0

Table 4: *Scores based on 2 categories ($p \leq 80\%$ and $p > 80\%$), hi=hits, fa=false alarm, mi=miss, cr= correct rejection.*

observations versus model predictions in an elaborated scatter plot (see Fig. 10). Up to 80 % PHEC has the superior score, but in the remaining part from 80 to 100 % PHEC underestimates the relative humidity. The other model versions have smaller biases and thus better results. Note that most of the members are located in this region. It is clear that PHEC is better in predicting small humidity amounts. To gain insight in misses and false alarms we have calculated scores based on contingency tables with two categories namely $p \leq 80\%$ and $p > 80\%$ (see Table 4). Also in terms of hits and misses in the $p \leq 80\%$ category PHEC has the best results, but again PHEC also has the highest false alarm rate.

3.2 Upper air verification

All radiosonde observations found present in the domain are used for verification. This is done to obtain more significant statistics. At 06 and 18 hours the number of observations is strongly reduced. Therefore they are excluded from the dataset.

- **Geopotential.** December 1999 (Fig. 4) shows an improvement of PHEC at the 850 and 500 hPa level. In contrast, the bias at the 250 hPa level degrades. During the May period (Fig. 7) there is hardly any difference between the model versions.

- **Wind speed.** Errors are generally larger in December 1999 than in May 2000 which is likely caused by the large number of storms that occurred in the winter month and the stronger winds on average. At the 250 hPa level PHEC has a negative bias and levels off, while the other model versions begin with a negative bias and have an upward trend which results in a change of sign of the bias. Note that the standard deviation of the bias is considerably larger in December than in May.

- **Temperature.** Conversely to the surface level all upper air levels show a positive temperature bias for both periods. Verification does not show much difference for both periods. The standard deviation is around 1K, while the bias approaches zero.

- **Dew point temperature.** Note the peculiar behavior at 250 hPa. The bias increases considerably with forecast period. The bias changes sign and the standard deviation levels off for two of the model versions.

3.3 Precipitation

3.3.1 55 km model

Precipitation forecasts have been verified using EWGLAM stations and a local raingauge network in Italy. Despite the limitations of this verification method i.e. double penalties for temporal and spatial error we expect to get an idea of the performance of the different models for the precipitation forecast. The EWGLAM stations cover a great part of Europe and the averaged distances of adjacent stations are about 100 kilometer (Fig. 1). Note that in this verification model results (that are an average over a large area) are compared with local observations. This is not fair comparison which degrades the scores.

In Fig. 11 on the top row the bias and standard deviation are presented. On the left and right panels the results for December 1999 and May 2000 are depicted. For both periods the standard deviation has the same order of magnitude of about 0.2 mm/6h. However the bias shows some differences. PHEC has the best score with a bias close to zero. December 1999 and May 2000 respectively show a positive and negative bias. December 1999 has a rapid increase of the bias in the time interval from 6 to 12 hours which is less pronounced during the May 2000. This increase is caused by the spin-up effect. The spin up in May 2000 is less than in December 1999 probably due to the difference in character of the precipitation in these periods. In December 1999 the total precipitation is dominated by large scale precipitation while in May 2000 the convective component is much larger. The latter is influenced less by spin up. There are no big differences between HL506 and HL514, which is not surprising since both models have the

same STRACO scheme. PHEC with the Tiedtke mass flux scheme and prognostic cloud scheme give slightly better results.

To get more insight in the performance of the models we have computed skill scores from the contingency tables with the following categories: $R > 0$ mm, $R \geq 0.3$ mm, $R \geq 1$ mm, $R \geq 3$ mm, $R \geq 10$ mm and $R \geq 30$ mm. In the contingency tables 6-hourly accumulations for all forecast lengths are used (see Table 5).

	o1	o2	o3	o4	o5	o6	o7	tot
f1	28/42/31	1/1/1	0/1/0	0/0/0	1/1/1	0/0/0	0/–/0	30/45/33
f2	23/16/22	2/2/2	2/2/2	1/1/1	0/0/0	0/0/0	0/0/0	28/22/27
f3	12/07/11	3/2/2	3/3/3	2/2/2	1/1/1	0/0/0	0/0/0	20/14/19
f4	03/03/05	1/1/1	3/3/3	3/2/2	2/2/2	0/0/0	0/0/0	14/12/14
f5	01/01/01	0/0/0	1/1/1	2/2/2	2/2/2	0/0/0	0/0/0	08/07/07
f6	00/00/00	0/0/0	0/0/0	0/0/0	0/0/0	0/0/0	0/–/0	01/00/00
f7	–	–	–	–	–	–	–	–
sum	69	7	10	7	6	1	0	100

Table 5: *Contingency table with percentages for December 1999 for the following sequence of model versions: HL506/PHEC/HL514. The categories are defined as follows:*$p = 0$, $0.0 < p \leq 0.3$, $0.3 < p \leq 1.0$, $1.0 < p \leq 3.0$, $3.0 < p \leq 10$, $10.0 < p \leq 30.0$ *and* $p > 30.0$ *mm. Note that – implies no occurrence, whereas 0 implies at least one occurrence.*

These seven-category contingency tables are transformed in 2 by 2 tables. This reduction method is schematically illustrated in Table 6. Based on these 2 by 2 contingency tables skill scores can be easily calculated. We focus here on the Bias-Ratio score (BRS) and Hanssen-Kuipers score (HKS)

	o1	o2	o3	o4	o5	o6
p1	d2	d2	c2	c2	c2	c2
p2	d2	d2	c2	c2	c2	c2
p3	b2	b2	a2	a2	a2	a2
p4	b2	b2	a2	a2	a2	a2
p5	b2	b2	a2	a2	a2	a2
p6	b2	b2	a2	a2	a2	a2

Table 6: *Reduction of a multi-category table into a 2 by 2 contingency table Example for* $\geq$ *category 2 a=hits, b=false alarms, c=miss, d=correct rejection. o=observations, p=predictions.*

$$BRS = \frac{a+b}{a+c} \tag{1}$$

$$HKS = \frac{ad-bc}{(a+b)(c+d)} \tag{2}$$

The BRS is the ratio of the number of yes forecasts to the number of yes observations. Unbiased forecasts exhibit BRS=1, indicating that the event was predicted the same number of times that it was observed. HKS is a skill score, implying that perfect forecasts receive a score of one, random forecasts receive a score of zero, and forecasts inferior to the random forecast receive negative scores. For further information see Kok [7] and Wilks [22].

In Fig. 11 the BRS, HKS and frequency distribution are given on the 2nd, 3rd and 4th row, respectively. From the frequency distribution it is clear that the "no rain" case is dominant. The underlying contingency tables are given (Table 5). Note that the extreme categories of $p > 10$ are hardly occurring. All model versions overestimate small precipitation amounts, which is a well known problem. PHEC has the best performance in terms of the BRS (2nd row) for both periods. In terms of HKS, which is depicted on the 3rd row, PHEC yields better results in December 1999, but slightly worse results in May 2000.

3.3.2 11 km model

So far all experiments have been carried out with a horizontal resolution of 0.5 degrees. We have also conducted experiments with a horizontal resolution of 0.1 degrees. The models were only modified in terms of domain, grid size and time step. The physics of the models were not affected. The models HL506 and PHEC were run for a rain event in Italy during 14 to 17 December 1999. We have been using data from a previous experiment (De Martino,[3]) and we begin here with a brief description of the synoptic situation.

A depression was developing over the Mediterranean Sea with an accompanying frontal system. The front moved from north to south over Italy. In Fig. 12 the front can be recognized by a jump in the wind and an extensive rain zone. Note that over the Tyrrenean Sea strong winds occur of more than 20 m/s, while over land variable weak winds prevail. Note also the small low pressure area in the Adriatic sea. Moist air was transported toward the coast and interacted with the Apennines mountains resulting in torrential rain over Campania. The maximum observed 6 hourly rainfall amounts were 93 mm. These details in the precipitation pattern were hardly detected by the EWGLAM stations because the spatial resolution of the network was insufficient. Therefore we used observations from a high resolution network of raingauges across Campania. Averaged distances of adjacent stations vary between 30 and 40 kilometer. A subjective comparison between the model reveals less precipitation amounts for HL506, which is confirmed by the scores.

In Fig. 13 the verification results of the high resolution raingauge network are given for the period of 14 to 17 December 1999. The 55 km models (left panel) reveal a large underestimation of precipitation and the 11 km models (right panel) show a significant reduction of the bias. Orographic forcing plays an important role in this case and in a 11 km model the orography is much finer resolvable, resulting in more realistic forcing. The standard deviation of PHEC slightly improves while HL506 deteriorates.

From the frequency distribution (4th row) it is clear that most observed amounts are found in between $p > 3$ and $p > 10$. This is confirmed by the contingency tables which are given in Table 7. The 55 km version of PHEC (left column of Fig. 13) reveals good

	o1	o2	o3	o4	o5	o6	o7	tot
f1	2.0/5.4	0.2/0.6	–/1.0	–/0.3	–/0.2	–/–	–/–	2.2/7.5
f2	1.4/2.0	0.6/0.6	0.7/0.8	0.2/0.8	0.3/1.0	–/0.1	–/–	3.2/5.2
f3	2.8/1.4	0.5/0.5	1.4/0.6	0.9/1.1	1.0/2.4	0.2/0.2	–/–	6.8/6.1
f4	3.3/1.2	1.7/1.4	1.1/1.7	4.4/3.6	7.1/5.6	2.5/1.8	0.4/–	20.5/15.4
f5	0.7/0.2	0.7/0.5	2.9/2.8	6.2/6.3	12.7/14.5	13.2/9.5	2.7/1.7	39.2/35.5
f6	–/–	–/–	0.8/0.1	5.2/4.6	11.8/8.4	7.8/11.8	1.8/2.6	27.4/27.5
f7	–/–	–/–	–/–	–/0.2	–/0.8	0.6/0.9	0.3/0.9	0.9/2.8
sum	10.2	3.6	6.9	16.8	32.8	24.3	5.2	100.0

Table 7: *Contingency table with percentages for 14-17 Dec 1999 for the Campania region, model versions HL506/PHEC, both 11km horizontal resolution . Categories are defined as follows:* $p = 0$, $0.0 < p \leq 0.3$, $0.3 < p \leq 1.0$, $1.0 < p \leq 3.0$, $3.0 < p \leq 10$, $10.0 < p \leq 30.0$ *and* $p > 30.0$ *mm.*

results with a BRS close to 1 for the small categories in combination with the highest values for HKS. In the 11 km runs, the precipitation forecasts from both model versions (right column of Fig. 13) obviously benefit from the increased detail in the orographic forcing owing to the finer horizontal resolution. Also the much smaller domain size (given the same number of gridpoints) will likely impose a stronger constraint on the synoptic-scale forcing in the region of interest closer to the observed large-scale flow, leaving fewer degrees of freedom for evolution of disturbances in the interior of the model domain. Also for the high-resolution runs PHEC has the better score for both BRS and HKS, especially in categories of the large precipitation amounts.

3.4 Other experiments

In this section we briefly discuss two more experiments that have been carried out for different reasons. The first experiment deals with the exchangeability of the radiation

scheme. The second experiment examines the application of a modified treatment of soil moisture in the ECMWF physics.

3.4.1 HIRLAM radiation and CPU demand

The radiation scheme from the ECMWF physical package is rather demanding on computing power. Therefore we made the additional effort to backsubstitute the HIRLAM radiation scheme into the physics package and tested the performance of PHEC with the "faster" radiation scheme. The results were found similar to the ones with the original radiation scheme. Again diurnal cycles in the bias resulted in evening out of positive and negative bias contributions. The gain in CPU demand due to back substitution of the HIRLAM radiation scheme appears to be modest. A single forecast time step with full ECMWF radiation needs about 3.3 times more CPU relative to a time step without full radiation. In the current set up full radiation is called only once an hour which reduces the gain in CPU demand to a factor 1.4 taking into account that HIRLAM radiation is a little more expensive than a quick update of radiative fluxes in the ECMWF code.

Table 8 provides an overview of the CPU demands required by the forecast components of the different model versions relative to the reference version HL506. In general, the forecast component of PHEC is found about 100% more expensive than HL506. Back substitution of HIRLAM radiation reduces this factor to about 55%. On the other hand, the forecast component of HL633, a very recent version of HIRLAM carrying essentially the same physics package as HL514 is about 45% more expensive than HL506. The net result is that the CPU demands of PHEC_HLRAD and more recent versions of HIRLAM (514 and later) are quite comparable, within 10% of each other.

model version	CPU demand
HL506	1.0
PHEC	$1.9 \sim 2.1$
PHEC_HLRAD	$1.5 \sim 1.6$
HL633	$1.4 \sim 1.5$

Table 8: *CPU demand of the forecast components of the different model versions relative to HL506. PHEC_HLRAD is PHEC, but with HIRLAM radiation backsubstituted. HL633 is a more recent version of HIRLAM for which the CPU demand of the forecast component is assumed comparable to version HL514. All model runs were carried out under MPI on 4 processors of the Sun-Fire-15000 at KNMI. (HL514 has never been ported to the KNMI system.)*

3.4.2 The role of soil moisture capacity

In this paragraph we discuss the application of the modified treatment of soil moisture in the ECMWF physics motivated by recent experience of running that package in a climate model RACMO2 (Lenderink et al., 2003). In particular, the model showed a tendency to (very) substantially overestimate near-surface summertime temperatures (up to +8 °C) across much of Central and Southern Europe associated with a strong reduction of the local hydrological cycle. A detailed analysis learned that this anomaly could, at least partly, be ascribed to the treatment of soil water in the land surface scheme. In particular, it was found that the total water holding capacity of the soil layer was insufficient to store the winter precipitation. The excess was carried away through runoff and thus lost as a source term for evaporation during spring and summer. The enhancement of the soil water reservoir with about 60 % together with a change in the response of vegetation to soil drying have indeed been found to greatly improve the RACMO2-simulation of the present-day summertime conditions across most of continental Europe. The enhancement of the soil water reservoir is not expected to have much impact on the model performance when operated in NWP-mode as it primarily affects the long-term response of the soil. However, the modification in the response of model vegetation to soil drying will affect the partitioning of the net surface radiative flux into sensible and latent heat fluxes, and hence result in different diagnoses for 2m temperature and humidity. The latter is only relevant in spring and summer conditions, in winter conditions there will be no effect at all. Results revealed that this assumption was correct. The changes were indeed rather small. A longer test period in summer conditions is required to show more significant differences.

4 Conclusions and discussion

ECMWF physics has been successfully ported into the HIRLAM system, version 5.0.6. HIRLAM 5.0.6 + ECMWF physics works well in December 1999 and shows better scores for surface and upper air parameters relative to the control experiment (HIRLAM 5.0.6). These promising results have been obtained without any change in the formulation of the ECMWF physics package. HIRLAM 5.1.4, carrying the ISBA-scheme, shows similar results, but the surface pressure is considerably worse. However another test period, May 2000, does not show substantial improvements for both HIRLAM 5.0.6 + ECMWF physics and HIRLAM 5.1.4 relative to standard HIRLAM 5.0.6., although the amplitude of the diurnal bias oscillation reduces slightly.

HIRLAM 5.0.6 + ECMWF physics works well on 0.5 and 0.1 degrees resolution. The physical parameterization is scalable, i.e. it can be applied without major modifications for 0.5 and 0.1 degrees resolutions. Compared to the HIRLAM 5.0.6 and HIRLAM 5.1.4 small rainfall amounts are less overestimated and large rainfall amounts tend to be less

underestimated. The Bias Ratio and Hanssen-Kuipers Score are useful tools to get more insight in the the performance of the models. Using a multi-category contingency table allows to focus on the distribution of the precipitation amount forecast.

All three model versions, but in particular the run based on HIRLAM 5.0.6, show a diurnal cycle in the bias of the 2m temperature and 10m wind speed. On the other hand, the amplitude of the diurnal cycle in the bias is found significantly reduced in HIRLAM 5.1.4, in particular close to analysis time. This result indicates that HIRLAM 5.1.4 greatly benefits from an ISBA compatible surface analysis component in the data-assimilation. However, for longer forecast times the skill of HIRLAM 5.0.6 + ECMWF physics is comparable or better, in particular in December 1999. In the current implementation (near) surface parameters are not assimilated in the HIRLAM 5.0.6 + ECMWF-physics version with the exception of sea surface temperature. To bring the HIRLAM 5.0.6 + ECMWF-physics performance at and close after analysis time to similar levels as the HIRLAM 5.1.4 scores requires a the development of a surface analysis scheme being compatible with the TESSEL surface scheme.

The enhancement of the soil water reservoir in the ECMWF-physics does not have much impact on the performance of HIRLAM 5.0.6 + ECMWF-physics when operated in NWP-mode as it primarily affects the long-term response of the soil. However, the modification in the response of model vegetation to soil drying will affect the partitioning of the net surface radiative flux into sensible and latent heat fluxes, and hence result in different diagnoses for 2m temperature and humidity. The latter is only relevant in spring and summer conditions, in winter conditions there will be no effect at all.

Backsubstitution of the HIRLAM radiation scheme in the version of HIRLAM 5.0.6 + ECMWF-physics yields results comparable with the version including the ECMWF radiation scheme, at least in the verification measure applied in this study. The CPU demand of the forecast component is found reduced by approximately 25% in the applied experimental setup.

5 Acknowledgements

Kees Kok (KNMI) is thanked for his help in interpreting the verification scores. The authors are indebted to Sander Tijm (KNMI) for his careful reading of an earlier version of the manuscript and for his valuable contribution during this research. Further we would thank Per Undén (SMHI) and an anonymous reviewer for their constructive comments on the draft of this report.

6 Appendix: Overview of Technical Implementation

In porting the ECMWF physics package the following strategy has been pursued.

1. To keep the components of the ECMWF physics modules untouched in order to facilitate the implementation of future releases.
2. To embed ECMWF physics variables in the HIRLAM code in a transparent way.
3. To build a separate interface between the HIRLAM dynamical core and the ECMWF physics in analogy with the existing PHCALL module.

Numerous changes were required to port the ECMWF physics package into the HIRLAM-system, as has been described in some detail in Newsletter 38 [9]. The majority of the modifications or additions are inserted at three distinct levels.

- In the forecast module
- In the scripts and makefiles
- In the generation of surface characteristics

Forecast module

The role of the interface modules is twofold. Their general task is to link the ECMWF physics with the dynamical core in the HIRLAM forecast module. Secondly, as ECMWF is coded in Fortran 90, while HIRLAM is still coded in Fortran 77, the interface routines have to relate global variables declared under F77 with auxiliary variables declared under F90, which makes explicit use of the KIND-function. This is done by copying information back and forth in order to ensure platform in-dependency.
For the reason mentioned above the number of changes in the ECMWF-physics is kept very limited. However, the number of changes applied to the HIRLAM code is relatively large, since it has to cope with a different set of parameters required and produced by the ECMWF physics package. A sizable portion of the changes can be distinguished in two major categories.

- ECMWF physics carries three prognostic cloud parameters, i.e. liquid water content, ice content, and cloud fraction. The HIRLAM reference version carries only one prognostic cloud parameter. To anticipate the use of three (or even more) prognostic cloud variables the present scalar element is extended by one dimension with size equal to the number of prognostic cloud variables. This modification is model independent and it would help enormously in porting the ECMWF physics in future HIRLAM releases when this modification is implemented in the HIRLAM reference system.

- The ECMWF physics employs a different set of surface and soil prognostic variables (different number of layers, different meaning of variables. etc.) and also quite different parameters to describe the surface characteristics (see section below on "Generation of Surface Characteristics"). Also a more extended set of output parameters is available. All together, the entire set of (near) surface and soil parameters is defined and kept as an entity. In future, on rephrasing the HIRLAM code into Fortran 90, such an entity could be considered a structure. In the present set up things are separated by means of a compiler directive (PH_ECMWF and PH_HIRLAM, respectively). This modification is model specific, but can be easily identified within the code.

Scripts and Makefile

A number of modifications are inserted in the various scripts in order to specify the necessary settings to operate the ECMWF physics. These include: i) defining the physics package and setting the corresponding compiler directive, ii) preparation of the relevant surface characteristics in the creation of climate files, iii) specification of name lists related to ECMWF-physics, and iv) making known the location of libraries corresponding to the ECMWF-physics. All modifications are brought under mini-SMS with the exception of the compilation of ECMWF-physics libraries. That is done a priori in standalone mode.

Generation of Surface Characteristics

ECMWF physics expects its own surface characteristics and as such a couple of additional fields need to be specified in the creation of climate files.

- The land surface scheme expects parameters to describe type and degree of low and high vegetation.
- In addition to the roughness length for momentum also a roughness length for heat is needed. It was given preference for reasons of consistency to prepare the roughness length fields according to the prescription in the IFS documentation [21]. As such the roughness length associated to vegetation prepared in the creation of climate files is blended with information on sub-grid scale orographic variance.
- The orographic wave drag scheme requires topographic information on the variance of terrain height, and, in addition, on anisotropy, mean slope, and direction of largest gradient. This is also taken care of in the creation of climate files.

In order to fully exploit the current experimental situation of having ECMWF physics as an option available in the HIRLAM system it is given into consideration to bring the ECMWF physics package and all necessary modifications into the HIRLAM reference

system. In that way it can be beneficial to the entire HIRLAM community. Such status also accommodates the implementation of future releases of the ECMWF physics package (or parts of it). To facilitate the implementation of ECMWF physics in future HIRLAM releases it is strongly recommended to convert the scalar prognostic cloud variable into an array variable suitable for a model-specific number of prognostic cloud parameters. It is desirable to recode the HIRLAM modules into Fortran 90. It will release some of the current overhead in the modules interfacing the ECMWF physics with the HIRLAM dynamical core. It also allows the user to specify the desired accuracy independently from the platform by means of the KIND-function. It finally offers the possibility to introduce structures which can be a very useful tool in generating transparent code, in particular in swapping information between subroutines.

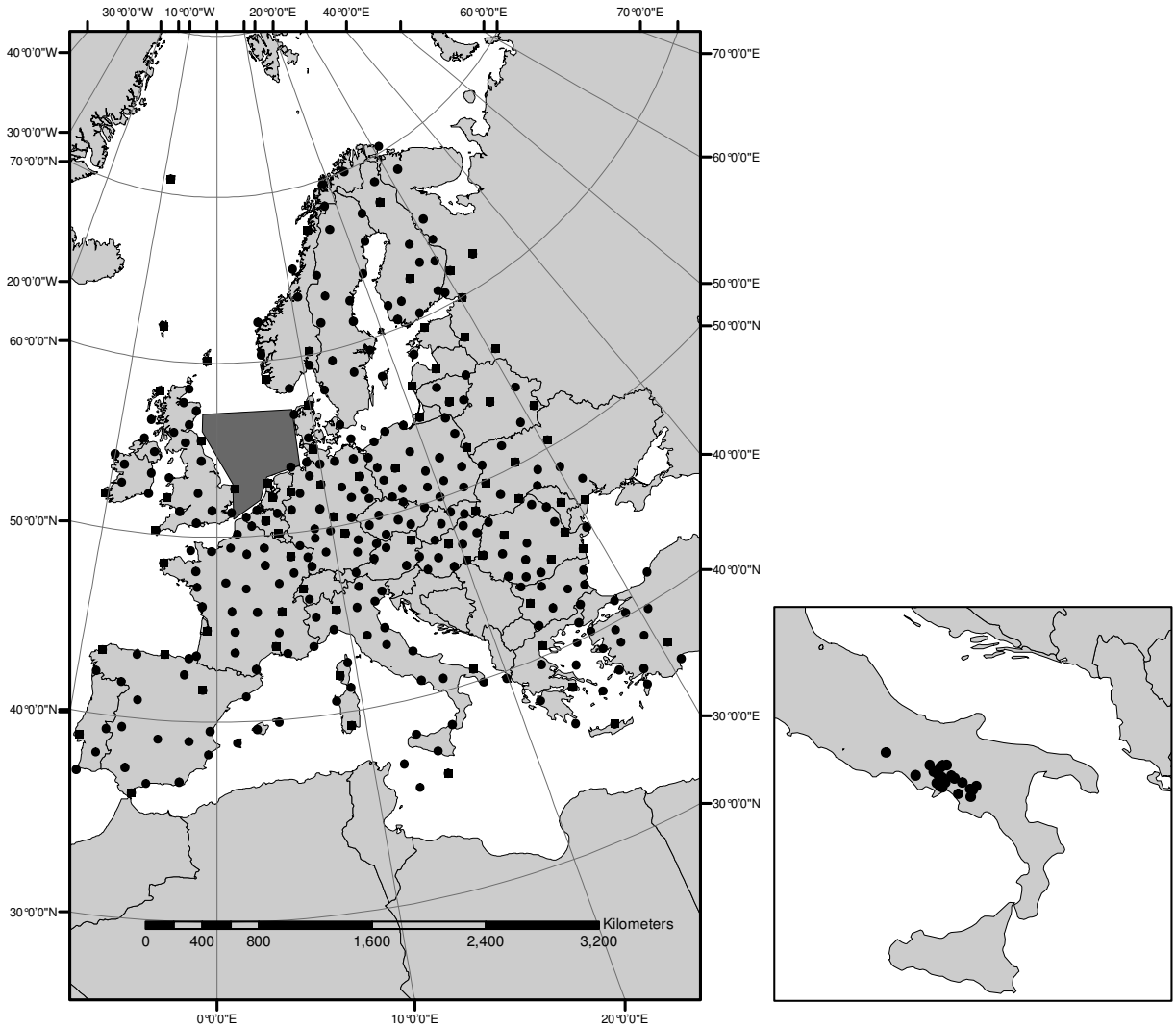

Figure 1: *EWGLAM stations and Southern North Sea (dark area) and local raingauges network in Campania Italy (right). SYNOP and temp stations are respectively dots and squares.*

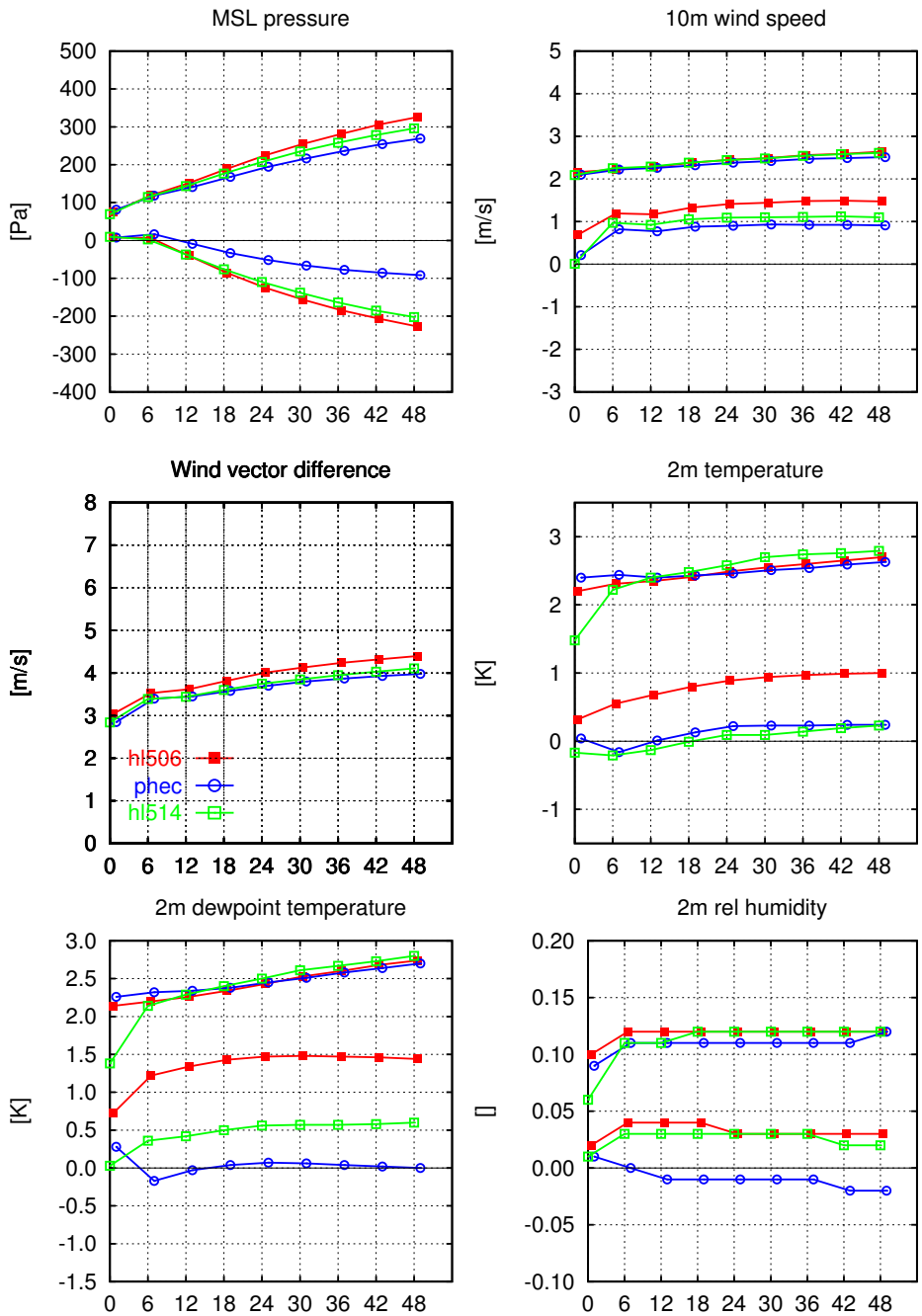

Figure 2: *EWGLAM station verification scores (standard deviation and bias) of near surface parameters as a function of the forecast length for the period 01-31 December 1999.*

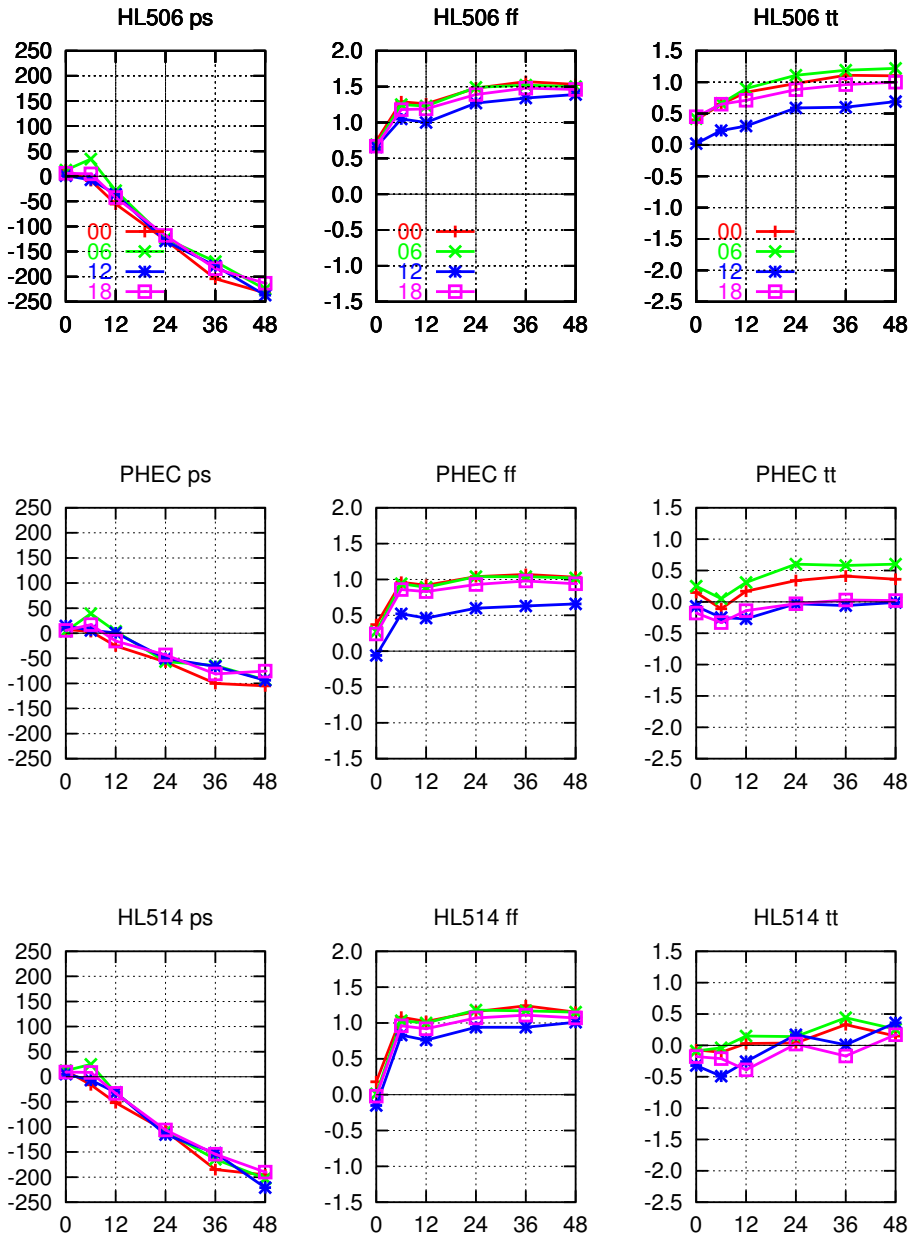

Figure 3: *Averaged bias during 01-31 December 1999 at synoptic hours as a function of forecast length for surface pressure (left), 10m wind speed (middle) and 2m temperature (right). Note that HL506, PHEC and HL514 are respectively depicted at the first, second and third row of the panels.*

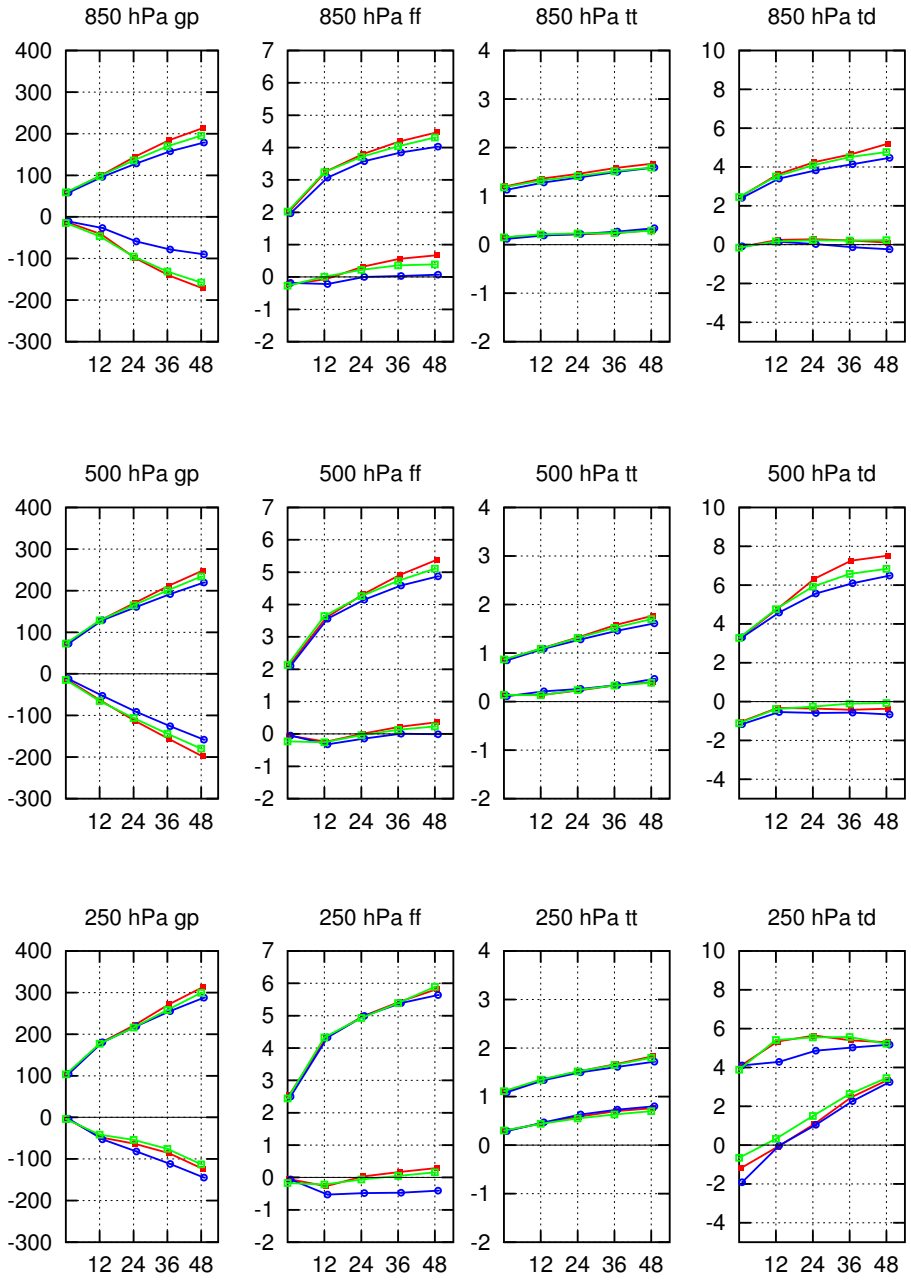

Figure 4: *Upper air verification during 01-31 December 1999 for all radiosonde stations in the domain. Note that gp is geopotential given in [J/kg], ff is wind speed [m/s], tt is temperature [K], td is dew point temp [K]. For explanation of curves see Fig. 2.*

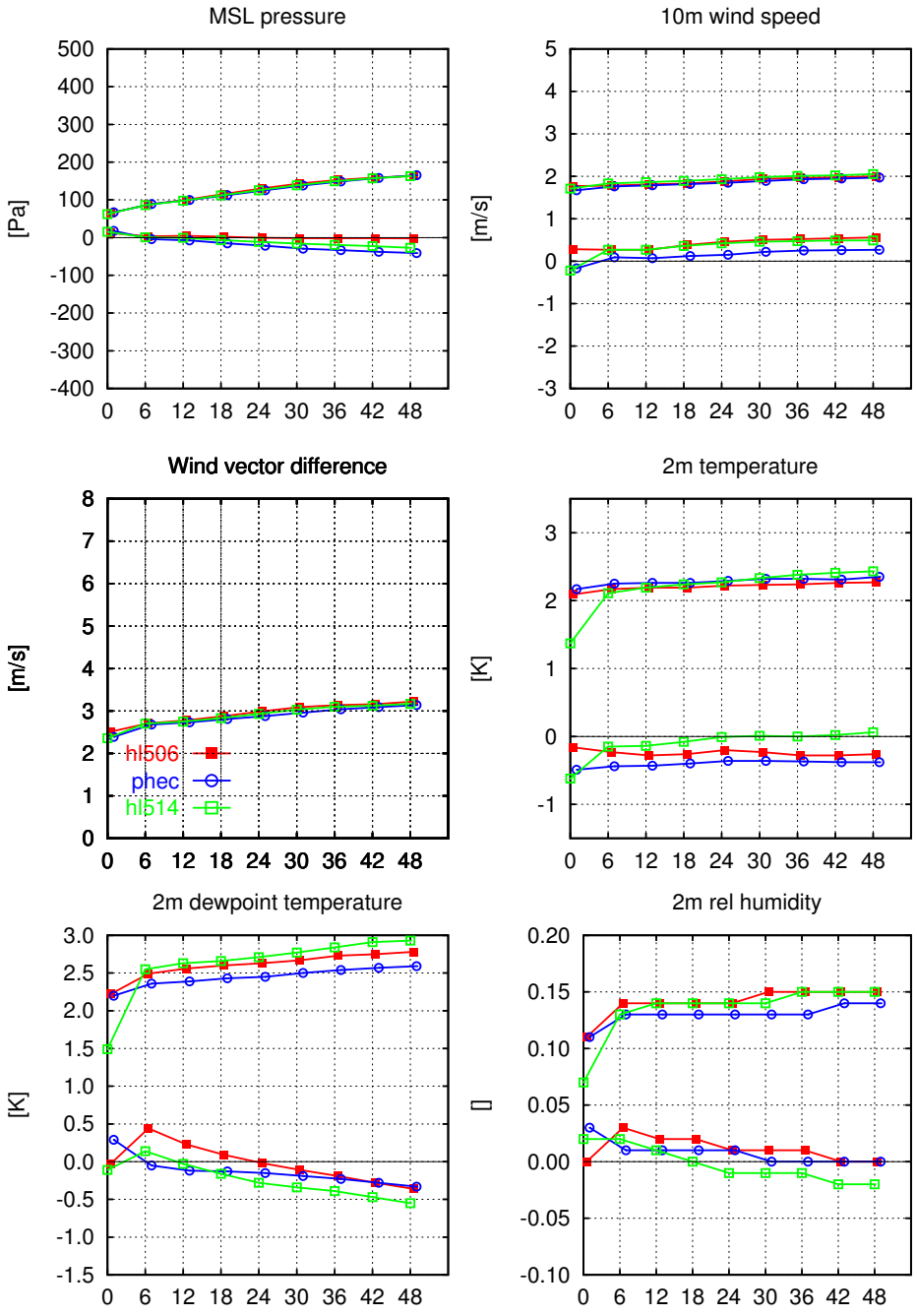

Figure 5: *Same as Fig. 2, but for 05-23 May 2000.*

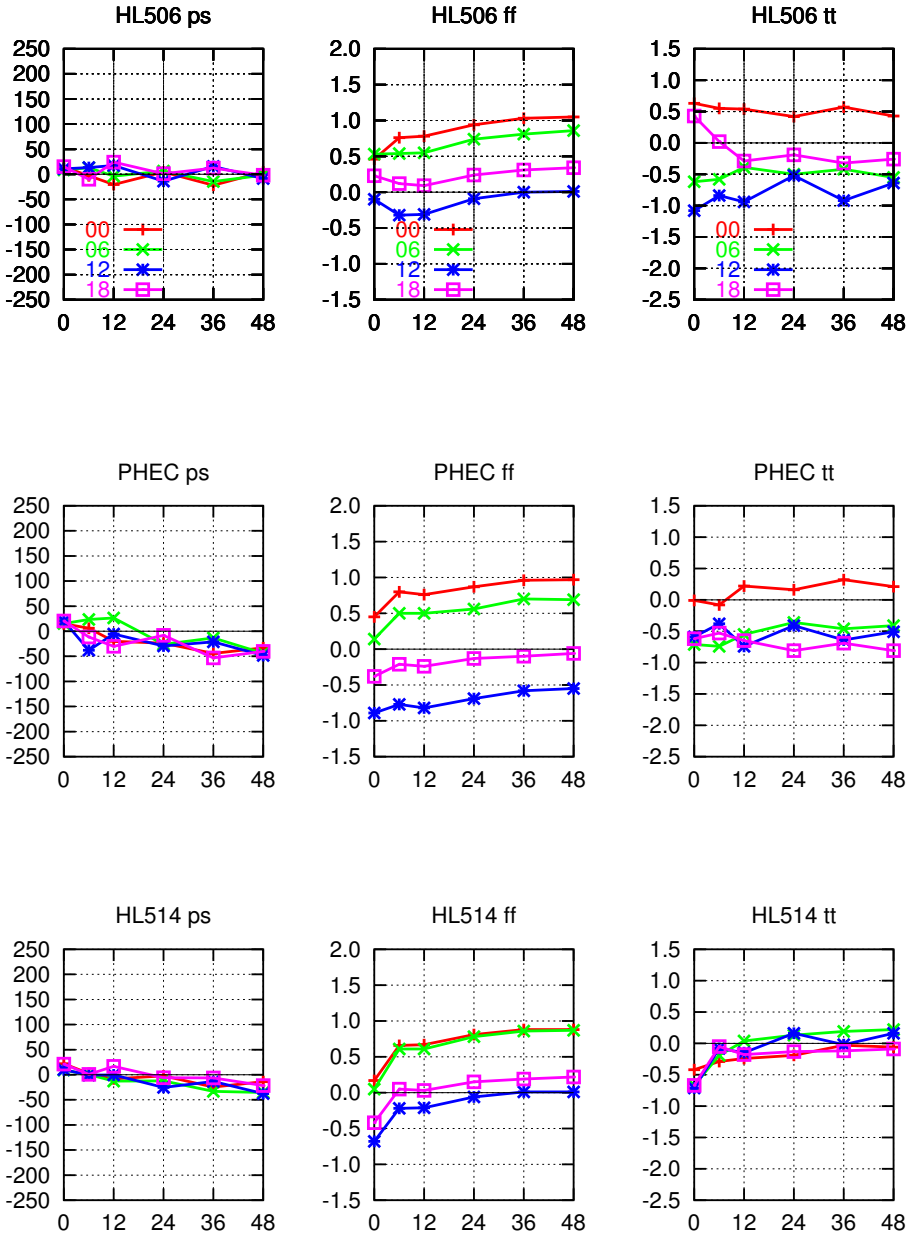

Figure 6: *Same as Fig. 3, but for 05-23 May 2000.*

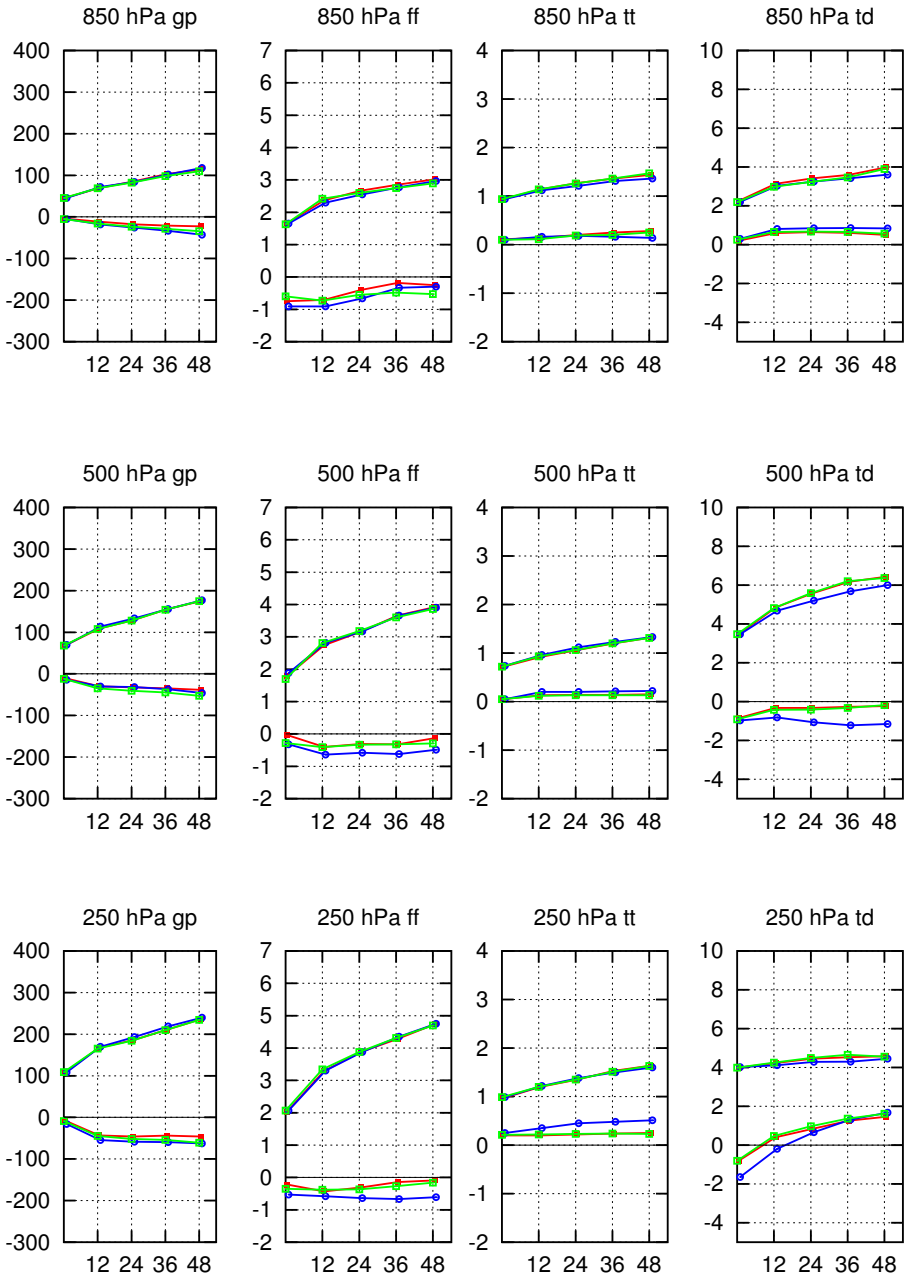

Figure 7: *Same as Fig. 4, but for 05-23 May 2000. For explanation of curves see Fig. 5.*

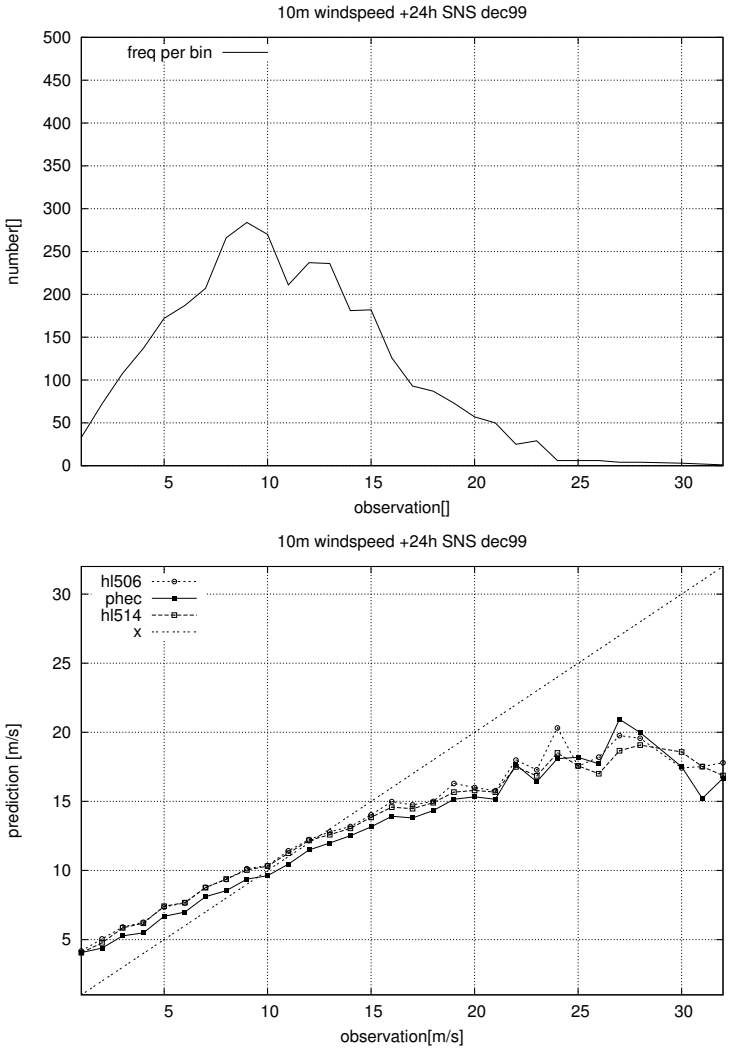

Figure 8: *The top panel shows a histogram of observed 10m wind speed during December 1999 for the Southern North Sea verification domain. The bottom panel shows the mean model predicted 10m wind speed from all three model versions as a function of the observed 10m wind speed. The curves are inferred from a scatter plot of synchronous and co-locating pairs of model predicted and observed 10m wind speed by averaging the model predicted values per interval of observed values (binning size 1 m/s).*

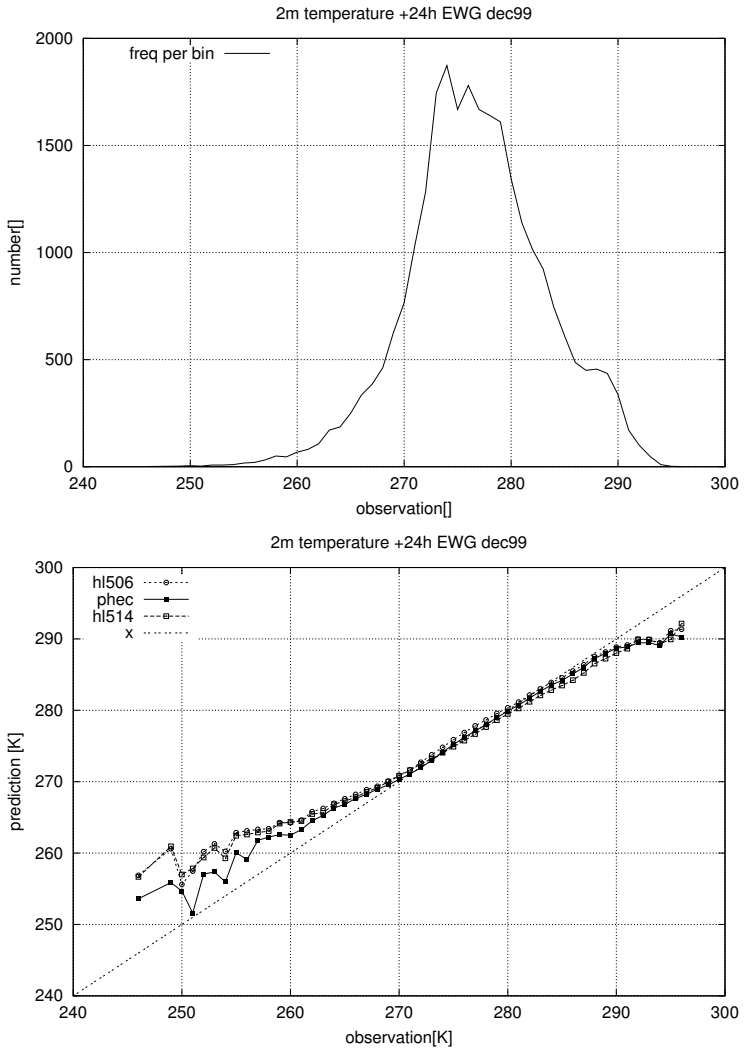

Figure 9: *Same as Fig. 8, but for 2m temperature and for EWGLAM stations. Observed temperatures are binned in intervals of 1 K width.*

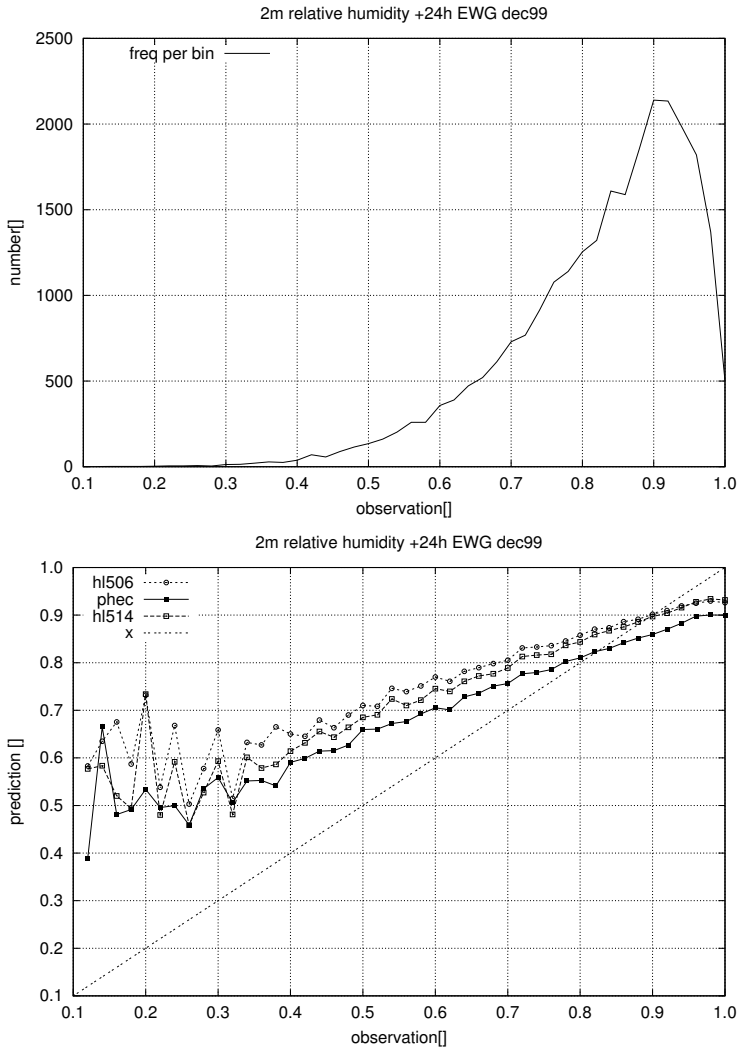

Figure 10: *Same as Fig. 8, but for 2m relative humidity and for EWGLAM stations. Observed relative humidities are binned in intervals of 2 % width.*

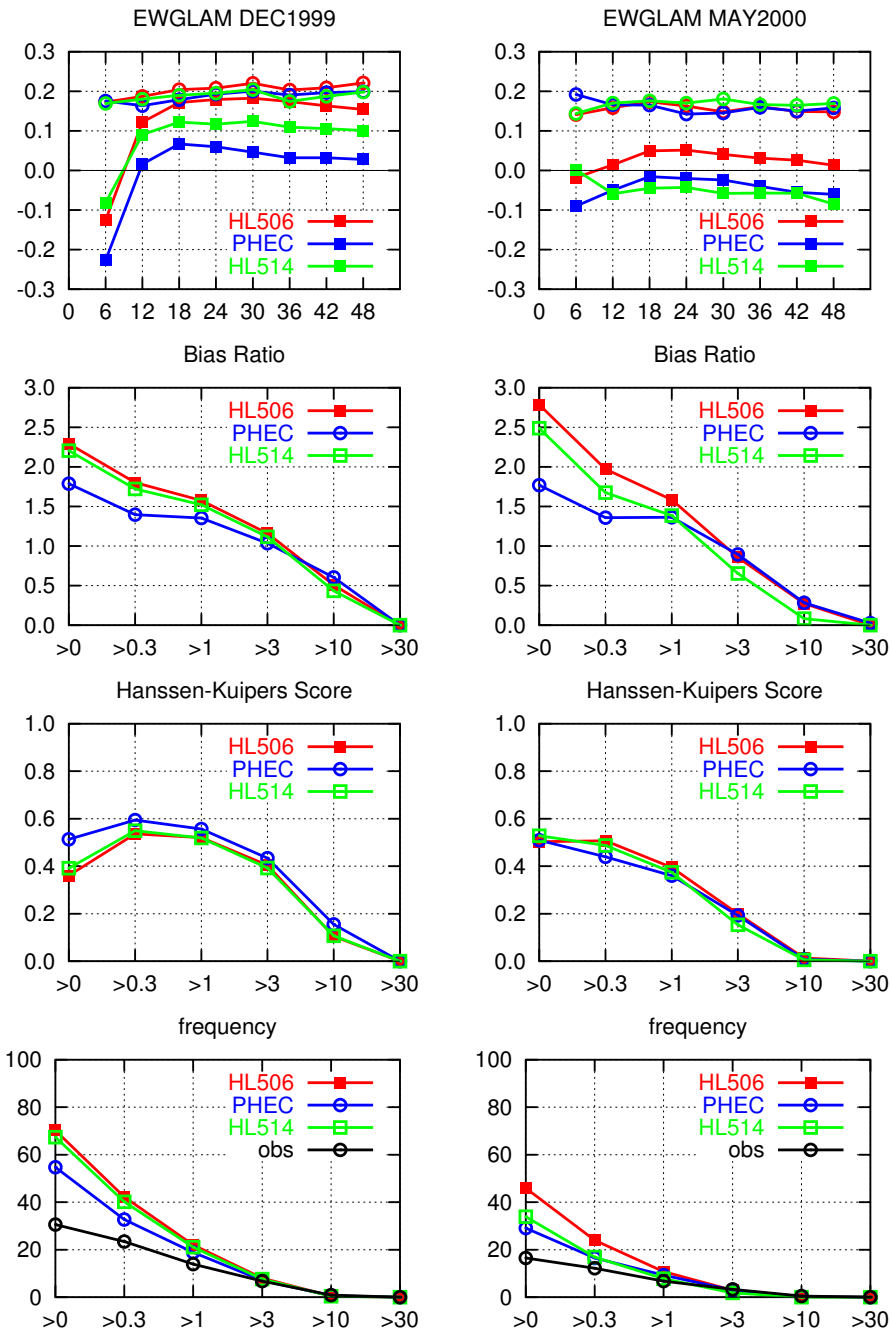

Figure 11: *Bias and standard deviation of precipitation forecasts (upper row), Bias Ratio Score (second row), Hanssen-Kuipers Score (third row), and frequency distributions (bottom row) for the EWGLAM stations for December 1999 (left column) and May 2000 (right column).*

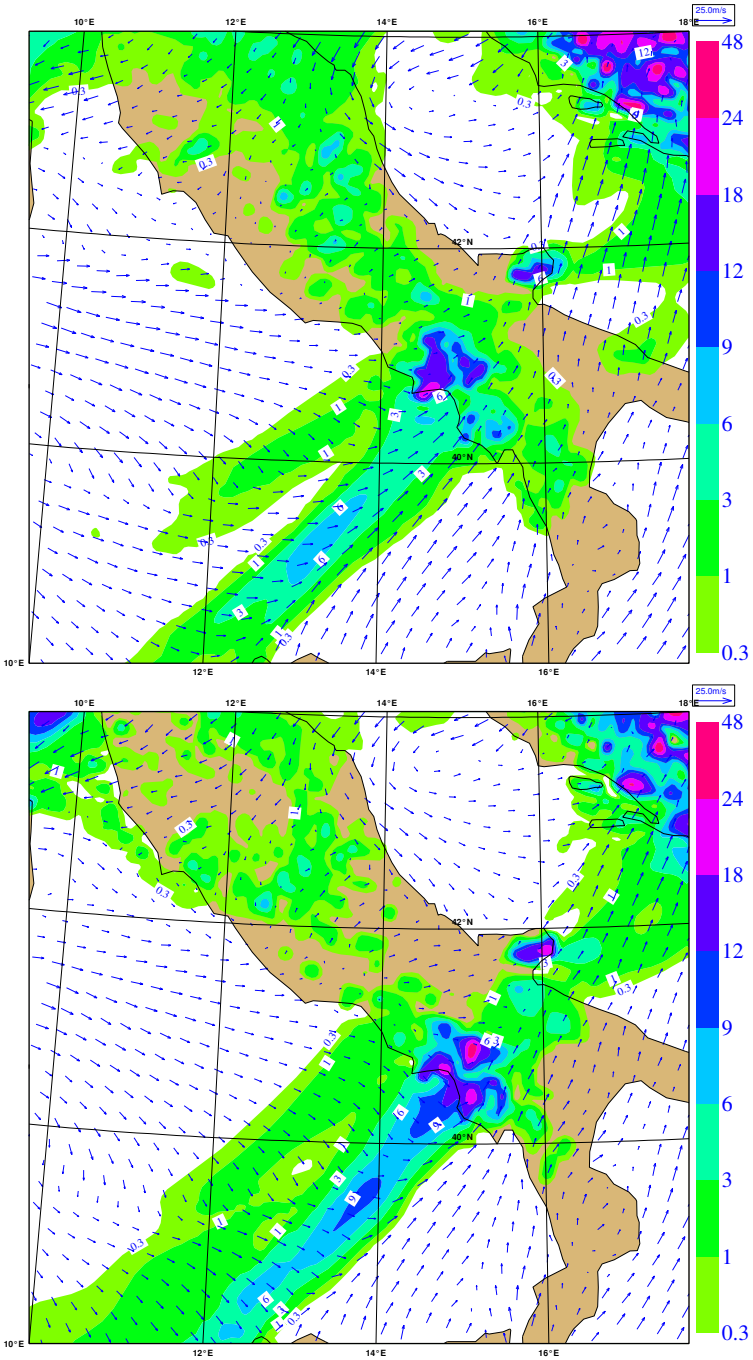

Figure 12: *Predicted 3-hour accumulated precipitation and 10m wind verifying on 16 December 1999, 0900 UTC for HL506 (up) end PHEC (below). Initial model time is 15 December 1999, 1200 UTC. Horizontal resolution is 11km.*

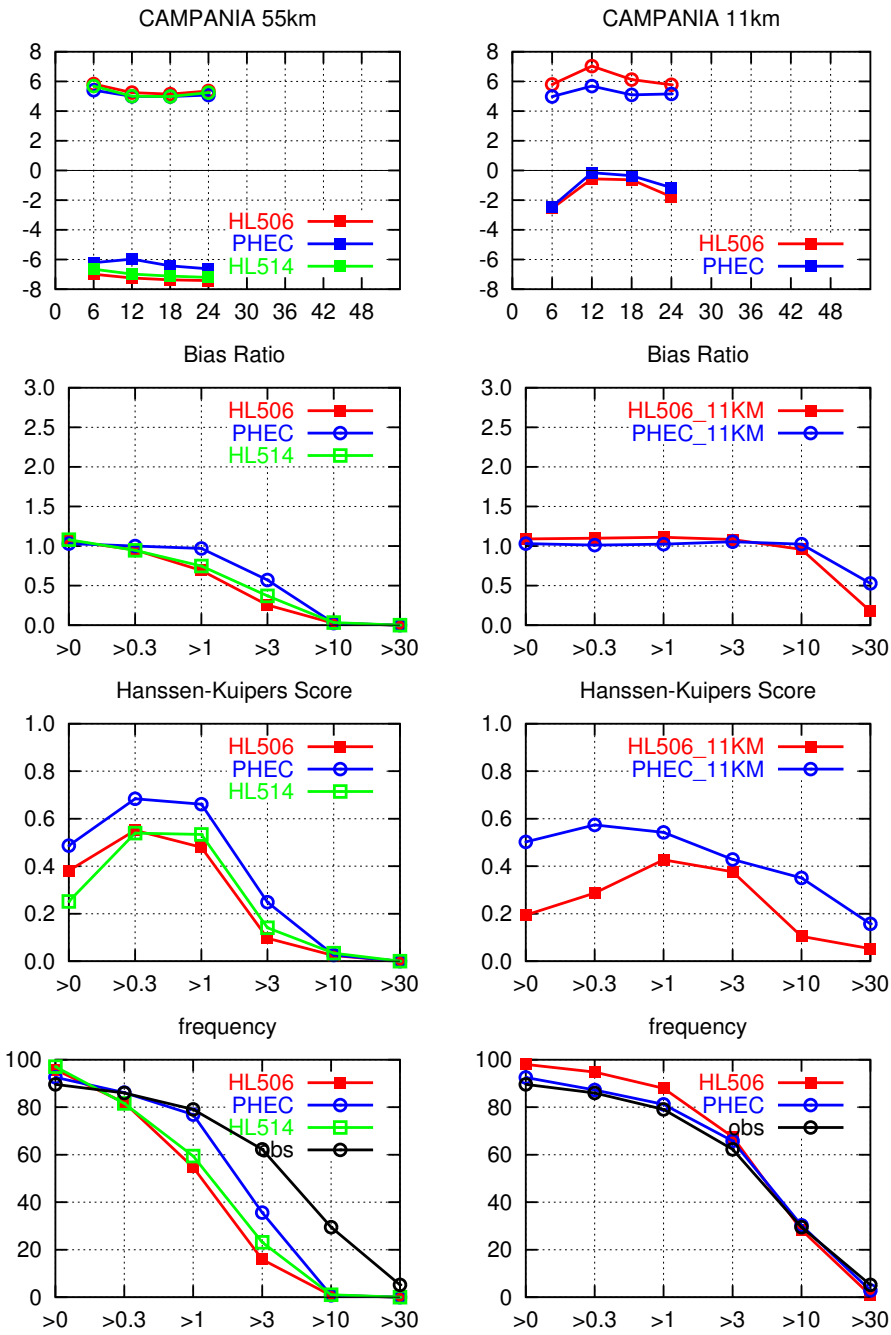

Figure 13: *Like Fig. 11, but for the Campania region during the period 14-17 December 1999. Left column shows results from coarse resolution runs (55 km), right column from high-resolution runs (11 km).*

References

[1] Baleste, M-C, Brunet, H., Mougel A., Coiffier J., Boudette, N., Bessemoulin, P., 2001: Les tempetes de Noel 1999. *Meteo France* **ISSN 1159-1056**

[2] Cuxart, J., P. Bougeault, and J.L. Redelsberger, 2000: A turbulence scheme allowing for mesoscale and large-eddy simulations. *Quart. J. Roy. Met. Soc.*, **126**, 1-30.

[3] De Martino, G., E, Pugliese Carratelli, E. Zambianchi, 2000: Application of the MM5 PSU/NCAR model to severe meteorological conditions in the Campania region. *Poster EGS meeting 2000*

[4] Lenderink, G., B.J.J.M van den Hurk, E. van Meijgaard, A.P. van Ulden and H. Cuijpers, 2003: Simulation of present-day climate in RACMO2: first results and model developments. *KNMI Technical Report* **252**, 24 p.

[5] Louis, J.F., 1979: A parametric model of vertical eddy fluxes in the atmosphere. *Boundary-Layer Meteorology,* **17**, 187-202

[6] Källén E. (editor), 1996: HIRLAM Documentation Manual System 2.5. SMHI. Norrköping. (Available from SMHI, S-601 76 Norrköping, Sweden).

[7] Kok, C.J., 2000: On the behavior of a few verification scores in yes/no forecasting *KNMI scientific report*, **WR-2000-04**,73p

[8] Kuo, H. L., 1965: On the formation and intensification of tropical cyclone through latent heat release by cumulus convection. *J. Atm. Sci.*, **22**, 40-63

[9] Meijgaard, E. van, 2001: ECMWF physics in HIRLAM. *Newsletter* **38** , 137-143.

[10] Morcrette, J-J, 1991, Radiation and cloud radiative properties in the ECMWF operational weather forecast model. *J. Geophys. Res.,* **96D**, 9121-9132.

[11] Noilhan, J., and J.-F. Mahfouf, 1996: The ISBA land surface parameterization scheme. *Global and Planetary Change*, **13**, 145-149

[12] Rodríguez, E, Beatriz Navascués, Juan José Ayuso, Simo Järvenoja, 2003: Analysis of surface variables and parameterization of surface processes in HIRLAM. Part I: Approach and verification by parallel runs. *HIRLAM Technical Report*, **58**, 52 p

[13] Rooy, Wim de, 2003: Modified roughness in ISBA and validation of CBR updates, *Hirlam Newsletter*, **44**.

[14] Sass, B.H., N.W. Nielsen, J.U. Jorgensen, B. Amstrup, 1999: The Operational DMI-HIRLAM system, *DMI Technical Report*, **99-21**, 42 p, (http://www.dmi.dk).

[15] Savijärvi, H., 1990: Fast radiation parameterization schemes for mesoscale and short-range forecast models. *J. Appl. Meteor.*, **29**, 437-447.

[16] Tiedtke, M, 1989: A comprehensive mass flux scheme for cumulus parameterization in large-scale models. *Mon. Weather Rev.* **117**, 1779-1800.

[17] Tiedtke, M, 1993: Representation of clouds in large-scale models. *Mon. Weather Rev.* **121**, 3040-3061.

[18] Tijm, A.B.C., 2003: Different aspects of CBR/CLJ, *Hirlam Newsletter*, **44**.

[19] Undén P. et al, 2002: HIRLAM-5 Scientific Documentation., 144p, (Available from SMHI, S-601 76 Norrköping, Sweden).

[20] Van den Hurk, B.J.J.M., P. Viterbo, A.C.M. Beljaars and A.K. Betts, 2000: Offline validation of the ERA40 surface scheme. *ECMWF Tech. Mem.* **295**, 42 pp.

[21] White, P.W. (editor), 2002: Physical processes (CY23R4). *IFS documentation http://www.ecmwf.int/research/ifsdocs.*

[22] Wilks, D. S. 1995: Statistical methods in the atmospheric sciences. *Academic Press*,464p